Article

Deducing the Energetic Cost of Protein Folding in Zinc Finger Proteins Using Designed Metallopeptides

Amit R. Reddi, Tabitha R. Guzman, Robert M. Breece, David L. Tierney, and Brian R. Gibney

J. Am. Chem. Soc., **2007**, 129 (42), 12815-12827• DOI: 10.1021/ja073902+ • Publication Date (Web): 29 September 2007

J|A|C|S
ARTICLES
Published on Web 09/29/2007

Deducing the Energetic Cost of Protein Folding in Zinc Finger Proteins Using Designed Metallopeptides

Amit R. Reddi,[†] Tabitha R. Guzman,[†] Robert M. Breece,[‡] David L. Tierney,[‡] and Brian R. Gibney*,[†]

Contribution from the Department of Chemistry, Columbia University, New York, New York 10027, and Department of Chemistry, University of New Mexico, Albuquerque, New Mexico 87131

Received May 30, 2007; E-mail: brg@chem.columbia.edu

Abstract: Zinc finger transcription factors represent the largest single class of metalloproteins in the human genome. Binding of Zn(II) to their canonical Cys_4, Cys_3His_1, or Cys_2His_2 sites results in metal-induced protein folding events required to achieve their proper structure for biological activity. The thermodynamic contribution of Zn(II) in each of these coordination spheres toward protein folding is poorly understood because of the coupled nature of the metal−ligand and protein−protein interactions. Using an unstructured peptide scaffold, **GGG**, we have employed fluorimetry, potentiometry, and calorimetry to determine the thermodynamics of Zn(II) binding to the Cys_4, Cys_3His_1, and Cys_2His_2 ligand sets with minimal interference from protein folding effects. The data show that Zn(II) complexation is entropy driven and modulated by proton release. The formation constants for Zn(II)-**GGG** with a Cys_4, Cys_3His_1, or Cys_2His_2 site are 5.6×10^{16}, 1.5×10^{15}, or 2.5×10^{13} M^{-1}, respectively. Thus, the Zn(II)-Cys_4, Zn(II)-Cys_3His_1, and Zn(II)-Cys_2His_2 interactions can provide up to 22.8, 20.7, and 18.3 kcal/mol, respectively, in driving force for protein stabilization, folding, and/or assembly at pH values above the ligand pK_a values. While the contributions from the three coordination motifs differ by 4.5 kcal/mol in Zn(II) affinity at pH 9.0, they are equivalent at physiological pH, $\Delta G = -16.8$ kcal/mol or a $K_a = 2.0 \times 10^{12}$ M^{-1}. Calorimetric data show that this is due to *proton-based* enthalpy−entropy compensation between the favorable entropic term from proton release and the unfavorable enthalpic term due to thiol deprotonation. Since protein folding effects have been minimized in the **GGG** scaffold, these peptides possess nearly the tightest Zn(II) affinities possible for their coordination motifs. The Zn(II) affinities in each coordination motif are compared between the **GGG** scaffold and natural zinc finger proteins to determine the free energy required to fold the latter. Several proteins have identical Zn(II) affinities to **GGG**. That is, little, if any, of their Zn(II) binding energy is required to fold the protein, whereas some have affinities weakened by up to 5.7 kcal/mol; i.e., the Zn(II) binding energy is being used to fold the protein.

Introduction

Metal-induced protein folding is an essential and ubiquitous process in Nature, enabling proteins to fold into specific three-dimensional structures for proper biological function.[1−5] Arguably, the most well studied class of proteins that exhibit this behavior are the zinc finger transcription factors.[6−11] Zinc finger proteins are typically unfolded in the *apo*-state and fold into well-defined structures competent for nucleic acid binding upon Zn(II) coordination to a Cys_4, Cys_3His_1, or Cys_2His_2 site. Since metal ion binding and protein folding are intimately coupled, the thermodynamic contribution of Zn(II) binding to each of these coordination motifs, as well as the amount of metal−ligand free energy used to drive protein folding, i.e., the cost of protein folding, are difficult to evaluate experimentally. Indeed, estimates of the cost of protein folding in zinc finger proteins range from 0 to +16 kcal/mol.[12−14] The ability to separate the thermodynamics of metal complexation from the cost of protein folding will address both the thermodynamic role of the metal in protein folding and the observation that all three canonical Zn(II) finger coordination motifs lead to similar K_d values at physiological pH values,[15] despite the fact that a Cys thiolate

[†] Columbia University.
[‡] University of New Mexico.

(1) Dyson, H. J.; Wright, P. E. *Curr. Opin. Struct. Biol.* **2002**, *12*, 54−60.
(2) Wittung-Stafshede, P. *Acc. Chem. Res.* **2002**, *35*, 201−208.
(3) Wilson, C. J.; Apiyo, D.; Wittung-Stafshede, P. *Q. Rev. Biophys.* **2005**, *3*, 1−30.
(4) Ghosh, D.; Pecoraro, V. L. *Curr. Opin. Chem. Biol.* **2005**, *9*, 97−103.
(5) Auld, D. S. *BioMetals* **2001**, *14*, 271−313.
(6) Cox, E. H.; McLendon, G. L. *Curr. Opin. Struct. Biol.* **2000**, *4*, 162−165.
(7) Frankel, A. D.; Berg, J. M.; Pabo, C. O. *Proc. Natl. Acad. Sci. U.S.A.* **1987**, *84*, 4841−4845.
(8) Berg, J. M. *Curr. Opin. Struct. Biol.* **1993**, *3*, 11−16.
(9) Schmiedeskamp, M.; Klevit, R. E. *Curr. Opin. Struct. Biol.* **1994**, *4*, 28−35.
(10) Matthews, J. M.; Sunde, M. *IUMB Life* **2002**, *54*, 351−355.
(11) Low, L. Y.; Hernandez, H.; Robinson, C. V.; O'Brien, R.; Grossmann, J. G.; Ladbury, J. E.; Luisi, B. *J. Mol. Biol.* **2002**, *319*, 87−106.
(12) Blaise, C. A.; Berg, J. M. *Biochemistry* **2002**, *41*, 15068−15073.
(13) Simpson, R. J. Y.; Cram, E. D.; Czolij, R.; Matthews, J. M.; Crossley, M.; Mackay, J. P. *J. Biol. Chem.* **2003**, *278*, 28011−28018.
(14) Okuda, M.; Tanaka, A.; Hanaoka, F.; Ohkuma, Y.; Nishimura, Y. *J. Biochem.* **2005**, *138*, 443−449.
(15) Payne, J. C.; Rous, B. W.; Tenderholt, A. L.; Godwin, H. A. *Biochemistry* **2003**, *42*, 14214−14224.

is a better ligand for Zn(II) than a His imidazole.[16−18] In addition, revelation of the fundamental thermodynamics of metal−ligand interactions in natural metalloproteins will provide for more predictable rational design of zinc proteins.[19−28]

Our approach to elucidating the free energy contributions of cofactor−protein interactions critical to biochemical function is to evaluate the affinity of cofactors for simplified *de novo* designed metallopeptides, or *maquettes*.[29] Using an analysis of the equilibria involved in the binding of metal and protons to the peptide scaffold, we have developed a methodology for determining the pH-independent formation constants, K_f^{ML} values, for designed metalloproteins.[30−32] In the case of heme proteins, this analysis parsed apart the thermodynamic contributions of the heme macrocycle−protein interactions and the heme iron−ligand interactions toward the overall free energy of heme−protein assembly.[32] This provided fresh insight into the structural factors responsible for proton-coupled electron-transfer events relevant to proton pumping enzymes such as cytochrome *c* oxidase. In the case of Zn(II) metallopeptides, our analyses of two unstructured 16 amino acid peptide ligands with four cysteine residues, **IGA**-Cys_4 and **GGG**-Cys_4, have demonstrated that Fe(II), Co(II), and Zn(II) binding to a Cys_4 site contributes −11.9, −15.8, and −22.1 kcal/mol in driving force for metalloprotein stabilization.[30,31] Additionally, calorimetric studies of Zn(II)-**GGG**-Cys_4 formation revealed that Zn(II) coordination is entropy driven, due to water release from both the peptide and the metal hydrate, and that the entropic driving force tracks with proton release.[31]

In this study, we utilize a minimal peptide model of a zinc finger protein, **GGG**, containing either a Cys_4, Cys_3His_1 or Cys_2His_2 binding site to elucidate the thermodynamic contribution of Zn(II) coordination. The unstructured, glycine-rich, 16-mer **GGG** peptide scaffold is designed to have minimal protein folding effects so as to provide the maximal Zn(II) affinities; i.e., the Zn(II) binding free energy is not being used to drive protein folding.[31] Fluorimetry, potentiometry, and calorimetry are employed to characterize the pH dependence of the thermodynamics of Zn(II) binding to the **GGG** variants. The data show that Zn(II) complexation by each coordination motif is entropy driven, due to dehydration of the peptide and metal upon complexation, as well as proton release. The data indicate that Zn(II)-Cys_4, Zn(II)-Cys_3His_1, and Zn(II)-Cys_2His_2 interactions can provide up to −22.8, −20.7, and −18.3 kcal/mol, respectively, in driving force for protein stabilization, folding, and/or assembly. While the contributions from these coordination motifs differ by 4.5 kcal/mol in Zn(II) affinity at pH 9.0, they are equivalent, at physiological pH, 7.4, $K_a = 2.0 \times 10^{12}$ M^{-1} or $\Delta G^{ML} = -16.8 \pm 1.0$ kcal/mol, due to proton competition for the thiolate ligands. A comparison of the Zn(II) affinities of each coordination motif between the **GGG** peptide scaffold and natural zinc finger proteins reveals that the cost of protein folding in the latter is minimal, i.e., less than +5.7 kcal/mol, if not zero. Furthermore, calorimetric data show *proton-based* enthalpy−entropy compensation (H^+-EEC) equalizes the free energies of Zn(II) binding at pH 7.4 for the three coordination motifs.

Experimental Section

Materials. Trifluoroacetic acid, ethanedithiol, 1-hydroxybenzotriazole, diethyl ether, acetic anhydride, diisopropylethylamine (DIEA), piperidine, cobalt(II) chloride, and zinc(II) chloride were obtained from Sigma-Aldrich. Natural Fmoc-protected amino acids were obtained from Bachem. HBTU, *O*-(1*H*-benzotriazole-1-yl)-*N*,*N*,*N*′,*N*′-tetramethyluronium hexafluorophosphate, was purchased from Qbiogene. All other chemicals and solvents were reagent grade and used without further purification. All peptide manipulations were performed under an inert atmosphere of dinitrogen.

Chemical Peptide Synthesis. The peptide ligands **GGG**-Cys_3His_1 and **GGG**-Cys_2His_2 were synthesized using solid-phase peptide synthesis and purified to homogeneity by reversed-phase HPLC in an analogous fashion to that reported for the prototype **GGG**-Cys_4 peptide ligand.[31] The sequences of each peptide are as follows:

GGG-Cys_4 NH_2-KL**C**EGG**C**GG**C**GG**C**GGW-$CONH_2$

GGG-Cys_3His_1 NH_2-KL**H**EGG**C**GG**C**GG**C**GGW-$CONH_2$

GGG-Cys_2His_2 NH_2-KL**H**EGG**H**GG**C**GG**C**GGW-$CONH_2$

Ultraviolet−visible−Near-Infrared (UV−vis−NIR) Spectroscopy. UV−vis spectra were recorded on either a Varian Cary 100 or 300 spectrophotometer using quartz cells of 1.0 cm path length. NIR spectra were recorded on a Perkin-Elmer Lambda 19 spectrophotometer. 1 mM NIR samples of the Co(II)-**GGG** complexes were prepared in 100% D_2O containing 20 mM HEPES, 100 mM KCl, pD = 7.5. All peptide concentrations were determined spectrophotometrically using an ϵ_{280} of 5600 M^{-1} cm^{-1} for Trp.

Fluorescence Spectroscopy. Excitation and emission fluorescence spectra were recorded on a Cary Eclipse fluorimeter using rectangular quartz cells of 1.0 cm path length. Excitation and emission slit widths of 5 nm were employed. pH titrations of the Zn(II)-**GGG** complexes were performed using an automated titrator attached to an AVIV 215 circular dichroism spectropolarimeter with a total fluorescence attachment. The excitation wavelength was 280 nm, and the total fluorescence emission was collected after a 310 nm high band-pass filter. The sample was maintained at 25 °C by a thermoelectric module with a ThermoNeslab refrigerated recirculating water bath as a heat sink. Peptide concentrations were between 10 and 50 μM.

Isothermal Titration Fluorimetry: Direct Zn(II) Titrations. Aqueous stock solutions of $Zn(II)Cl_2$ were added in microliter aliquots to freshly prepared peptide solutions in aqueous buffers (20 mM MES, 100 mM KCl) under strictly anaerobic conditions in 1.0 cm cuvettes. Samples were allowed to equilibrate for 3 min before measurement of their fluorescence spectra. The conditional metal−ligand dissociation constants, conditional K_d values, were obtained from fitting a plot of the increase in tryptophan fluorescence at 355 nm against the [Zn(II)]/[Peptide] ratio to a 1:1 equilibrium binding model described in the Supporting Information.

(16) Gockel, P.; Vahrenkamp, H.; Zuberbühler, A. D. *Helv. Chim. Acta* **1993**, *76*, 511−520.
(17) Vogler, R.; Vahrenkamp, H. *Eur. J. Inorg. Chem.* **2002**, 761−766.
(18) Vallee, B. L.; Auld, D. S. *Acc. Chem. Res.* **1993**, *26*, 543−551.
(19) Regan, L.; Clarke, N. D. *Biochemistry* **1990**, *29*, 10878−10883.
(20) Krizek, B. A.; Amann, B. T.; Kilfoil, V. J.; Merkle, D. L.; Berg, J. M. *J. Am. Chem. Soc.* **1991**, *113*, 4518−4523.
(21) Handel, T. M.; Williams, S. A.; DeGrado, W. F. *Science* **1993**, *261*, 879−885.
(22) Struthers, M. D.; Cheng, R. P.; Imperiali, B. *Science* **1996**, *271*, 342−345.
(23) Struthers, M. D.; Cheng, R. P.; Imperiali, B. *J. Am. Chem. Soc.* **1996**, *118*, 3073−3081.
(24) Dahiyat, B. I.; Mayo, S. L. *Science* **1997**, *278*, 82−87.
(25) Wisz, M. S.; Garrett, C. Z.; Hellinga, H. W. *Biochemistry* **1998**, *37*, 8269−8277.
(26) Pabo, C. O.; Peisach, E.; Grant, R. A. *Annu. Rev. Biochem.* **2001**, *70*, 313−340.
(27) Ambroggio, X. I.; Kuhlman, B. *J. Am. Chem. Soc.* **2006**, *128*, 1154−1161.
(28) Dhanasekaran, M.; Negi, S.; Sugiura, Y. *Acc. Chem. Res.* **2006**, *39*, 45−52.
(29) Robertson, D. E.; Farid, R. S.; Moser, C. C.; Urbauer, J. L.; Mulholland, S. E.; Pidikiti, R.; Lear, J. D.; Wand, A. J.; DeGrado, W. F.; Dutton, P. L. *Nature* **1994**, *368*, 425−432.
(30) Petros, A. K.; Reddi, A. R.; Kennedy, M. L.; Hyslop, A. G.; Gibney, B. R. *Inorg. Chem.* **2006**, *45*, 9941−9958.
(31) Reddi, A. R.; Gibney, B. R. *Biochemistry* **2007**, *46*, 3745−3758.
(32) Reddi, A. R.; Reedy, C. J.; Mui, S.; Gibney, B. R. *Biochemistry* **2007**, *46*, 291−305.

Table 1. pK_a Values for *apo*- and *holo*-Peptides as Determined from Potentiometric pH Titrations

	Cys_4		Cys_3His_1		Cys_2His_2	
titratable residues	*apo*	*holo*	*apo*	*holo*	*apo*	*holo*
Glu_4	4.8	4.6	4.5	4.7	4.8	4.5
His	NA	NA	6.5	3.1	6.5	3.0
His	NA	NA	NA	NA	6.9	3.2
Cys	7.8		NA	NA	NA	NA
Cys	8.1	5.0	8.1		NA	NA
Cys	8.7		8.6	5.6	8.8	5.6
Cys	9.0	5.6	9.0		9.1	
N-terminus	9.6	9.5	9.8	9.7	10.1	10.2
Lys_1	10.5	10.8	10.9	10.8	10.4	10.6

Isothermal Titration Fluorimetry: EDTA Competition Titrations. For pH values above 6.0, conditional equilibrium dissociation constant determinations for the Zn(II)-**GGG**-Cys_3His_1 and Zn(II)-**GGG**-Cys_2His_2 complexes necessitated the use of ethylenediaminetetraacetic acid, EDTA, competition. To buffered aqueous solutions (20 mM HEPES, 100 mM KCl) of 10−15 μM peptide and 1.0 equiv of Zn(II), EDTA was titrated in microliter aliquots under strictly anaerobic conditions. The decrease in fluorescence at 355 nm upon the addition of EDTA is fit to a competition model described in the Supporting Information. The K_{comp} value, derived from the nonlinear least-squares fitting of the competition titration data, was coupled with the conditional equilibrium dissociation constant value of Zn(II)-EDTA,[33] to yield the conditional equilibrium dissociation constant values for the Zn(II)-**GGG**-Cys_3His_1 and Zn(II)-**GGG**-Cys_2His_2 complexes.

Potentiometric pH Titrations. Potentiometric pH titrations of both *apo* and *holo*-**GGG**-Cys_3His_1 and **GGG**-Cys_2His_2 were performed using a 1.0 cm path length cuvette fitted with a pH electrode under a stream of nitrogen gas. The change in solution pH was monitored by a combination electrode upon addition of microliter aliquots of standardized 0.1 N HCl to an aqueous solution of 100 μM peptide containing 100 mM KCl at a pH value of 12.0. As described previously for **GGG**-Cys_4, the *apo*-peptide titration data were best fit to a protonation model involving the ionization of seven ionizable residues, i.e., the N-terminus, Lys_1, Glu_4, and the four ligand residues.[31] The previous ligand pK_a assignments of the **GGG**-Cys_4 peptide, given in Table 1, are supported by the *apo* and *holo* **GGG**-Cys_3His_1 and **GGG**-Cys_2His_2 peptide data. In the case of the *apo*-peptides, only the Cys to His alterations result in significant changes in the observed pK_a values. In the case of the *holo*-peptides, the effective pK_a values of the ligand residues shift due to metal-ion competition, while those not directly involved in metal-ion binding possess similar pK_a values to the *apo*-peptide.

Since tryptophan fluorescence is effected by the protonation state of cysteine,[34] we measured the pH dependence of the fluorescence of the Zn(II)-**GGG** complexes to determine the cysteine pK_a^{eff} values. As shown in the Supporting Information, the fluorescence intensity as a function of solution pH was best fit to protonation models involving a cooperative three proton transition and a separate one proton transition for Zn(II)-**GGG**-Cys_4, a cooperative three proton transition for Zn(II)-**GGG**-Cys_3His_1, or a cooperative two proton transition for Zn(II)-**GGG**-Cys_2His_2. The cysteine pK_a^{eff} values determined by fluorescence match those determined from the potentiometric titrations within a 0.1 pH unit error and confirm the pK_a^{eff} value assignments in Table 1.

pH Dependence of Conditional Dissociation Constants. Due to the expected pH dependence of the Zn(II)-**GGG**-Cys_3His_1 and Zn(II)-**GGG**-Cys_2His_2 conditional dissociation constants, K_d values for each were measured at varying pH values in order to determine the values of their pH-independent formation constants, K_f^{ML}. The K_d value at each pH was determined as above using fluorescence spectroscopy. The resulting plots of $-\log K_d$ versus pH are fit to equilibrium binding expressions, described in the Supporting Information, that take into consideration the ligand pK_a and pK_a^{eff} values, the solution pH and the pH independent formation constant, K_f^{ML}, for each Zn(II)−peptide complex.[31,35]

Isothermal Titration Calorimetry (ITC). ITC experiments were performed on a MicroCal OMEGA titration calorimeter. Typical experiments involved the titration of microliter aliquots of a 5.0 mM buffered stock solution of $Zn(II)Cl_2$ into matched buffered solutions of 25−75 μM peptide.[36−39] Below pH values of 9.0, the $Zn(II)Cl_2$ stock is predominantly $\{Zn(II)(H_2O)_6\}^{2+}$ and hydrolysis does not occur to a significant extent.[40,41] All peptide manipulations were done anerobically, and all solvents were thoroughly degassed to prevent cysteine oxidation. The sample was maintained at 25 °C by using a ThermoNeslab refrigerated recirculating water bath as a heat sink. Titrations were conducted in triplicate using three different buffers at each of three pH values, 5.5, 7.0, and 8.0. At all pH values 20 mM HEPES, 100 mM KCl ($\Delta H_{protonation} = -5.02$ kcal/mol)[42] and 20 mM PIPES, 100 mM KCl ($\Delta H_{protonation} = -2.73$ kcal/mol)[42] were used. At pH 8.0, 20 mM MOPS, 100 mM KCl ($\Delta H_{protonation} = -5.22$ kcal/mol)[42] was also employed, while at pH 5.5 and 7.0, 20 mM MES, 100 mM KCl ($\Delta H_{protonation} = -3.71$ kcal/mol)[42] was used. At pH 7.0 (20 mM HEPES, 100 mM KCl), titrations were completed at 25, 35, and 65 °C in order to determine ΔC_P values for each Zn(II)−peptide complex. Between each experiment, the sample cell was thoroughly rinsed with 0.1 M EDTA, followed by deionized water, to ensure complete removal of residual metal salts, EDTA, and peptide. The solution pH was checked before and after each experiment to ensure that there were no changes in pH.

All data were analyzed using the Origin software supplied with the MicroCal instrument. All data showed the expected 1:1 metal/peptide stoichiometry, consistent with the lack of hydrolysis or precipitation of the $\{Zn(II)(H_2O)_6\}^{2+}$ stock solution. Prior to fitting to a 1:1 equilibrium binding model, heats of dilution, derived from control experiments, were subtracted from the experimental data. The reaction enthalpies were determined according to the following relationship:

$$\Delta H_{obs} = \Delta H_{rxn} + n\Delta H_{buffer\ protonation} \quad (1)$$

where ΔH_{obs} is the observed enthalpy, ΔH_{rxn} is the intrinsic reaction enthalpy, $\Delta H_{buffer\ protonation}$ is the enthalpy of buffer protonation, and n is the number of protons released upon metal binding. The intrinsic reaction enthalpy and the number of protons released were determined using two methods, Method A and Method B. In Method A, ΔH_{rxn} and n were found by determining the y-intercept and slope, respectively, of a plot of ΔH_{obs} vs $\Delta H_{buffer\ protonation}$ from a linear regression analysis. The error on the ΔH_{rxn} and n values at every pH is the standard error of each sample set. In Method B, ΔH_{rxn} was determined by setting n equal to the value calculated based on the speciation of the ligand and metal ligand complex as determined from the potentiometric pH titrations shown in Table 1. The reported value of ΔH_{rxn} in this case is the mean of all the trials under the various buffer conditions, and the error is the standard deviation. Both methods gave identical results, within the error of the measurements, and are compared in the Supporting Information. For simplicity, all ΔH_{rxn} and n values reported in the text of the manuscript are calculated according to Method B. The reaction entropies were calculated based on the calorimetric

(33) Martell, A. E.; Smith, R. M. *Critical Stability Constants*; Plenum Press: New York, 1974.
(34) Harris, H. L.; Hudson, B. S. *Biochemistry* **1990**, *29*, 5276−5285.
(35) Magyar, J. S.; Godwin, H. A. *Anal. Biochem.* **2003**, *320*, 39−54.
(36) Wiseman, T.; Williston, S.; Brandts, J. F.; Lin, L. N. *Anal. Biochem.* **1989**, *179*, 131−137.
(37) Freire, E.; Mayorga, O.; Straume, M. *Anal. Biochem.* **1990**, *62*, 950A−959A.
(38) Ladbury, J. E.; Chowdhry, B. Z. *Chem. Biol.* **1996**, *3*, 791−801.
(39) Zhang, Y.; Akilesh, S.; Wilcox, D. E. *Inorg. Chem.* **2000**, *39*, 3057−3064.
(40) Richens, D. T. *The Chemistry of Aqua Ions*; John Wiley & Sons: New York, 1997.
(41) Zhu, M.; Pan, G. *J. Phys. Chem. A* **2005**, *109*, 7648−7652.
(42) Fukada, H.; Takahashi, K. *Proteins* **1998**, *33*, 159−166.

determination of the reaction enthalpies and the reaction free energies, ΔG_{rxn}, according to the following expression:

$$\Delta G_{rxn} = \Delta H_{rxn} - T\Delta S_{rxn} \quad (2)$$

The values of ΔG_{rxn} used in eq 2 were determined directly from ITC, where available, or from the analogous fluorimetric titration data.

X-ray Absorption Spectroscopy: Samples for EXAFS (1−2 mM, pH = 7.5) were prepared with 30% (v/v) glycerol as a cryoprotectant, preloaded in Lucite cuvettes with 6 μm polypropylene windows, and frozen rapidly in liquid nitrogen. XAS data were measured at the National Synchrotron Light Source (NSLS), beamline X3B, using a Si (111) double crystal monochromator and a Ni focusing mirror for harmonic rejection. Data collection and reduction were performed according to published procedures.[43] X-ray absorption spectra for Zn(II)-**GGG**-Cys_4, Zn(II)-**GGG**-Cys_3His_1, and Zn(II)-**GGG**-Cys_2His_2 were measured on individually prepared samples (8 scans per sample).

The resulting $\chi(k)$ EXAFS data were fit using the nonlinear least-squares algorithm contained in the program IFEFFIT, interfaced with SixPack.[44] In all fits, the coordination number was varied in one-quarter steps,[45] while the scale factor, S_c, and ΔE_0 were held fixed at calibrated values (Zn: $\Delta E_0 = -21$ eV, $S_{Zn-N} = 0.78$; $S_{Zn-S} = 0.87$), allowing only the distance (R_{as}) and the Debye−Waller factor (σ^2_{as}) to float. The fits presented were generated for Fourier filtered data; fits to unfiltered data gave similar results. Multiple-scattering contributions from histidine ligands were approximated by fitting FEFF calculated paths to the experimental EXAFS, as described previously.[45,46] The uncertainty in the number of imidazoles, determined in this way, is estimated to be ±0.5.

Results

Experimental Design. Zinc finger proteins are the classic examples of biological macromolecules that undergo metal-induced protein folding events.[6−11] Devoid of well-defined structural elements in the *apo*-state, zinc fingers fold into discreet three-dimensional structures upon Zn(II) complexation. Scheme 1A shows an archetypical zinc finger transcription factor, Zif268,[47] and a free energy diagram of a coupled metal-induced protein folding event in which the *apo*-protein populates the ensemble of *apo*-unfolded states that are lower in energy than the *apo*-folded state and in which the holo-protein populates the *holo*-folded state. The free energy required to fold the *apo*-protein into the *apo*-folded state, i.e., the structure observed in the *holo*-protein but without the metal bound, is given by $\Delta G_{apo}^{folding}$. The conditional dissociation constant, K_d value, measured for the transition from the ensemble of *apo*-unfolded states to the *holo*-folded state upon metal-ion binding can be used to determine the observed metal−ligand binding free energy, ΔG^{ML-Obs}, via the relationship $\Delta G^{ML-Obs} = -RT \ln K_d$. However, the *observed* free energy of metal binding, ΔG^{ML-Obs}, is less than the *actual* metal−ligand free energy contribution, ΔG^{ML}, by the cost of protein folding, $\Delta G_{apo}^{folding}$, i.e., $\Delta G^{ML} = \Delta G^{ML-Obs} - \Delta G_{apo}^{folding}$. While it is difficult to separate the energetics of protein folding from metal-ion binding, literature estimates for $\Delta G_{apo}^{folding}$ range from 0 to +16 kcal/mol.[12−14]

Scheme 1 Free Energy Diagram[a]

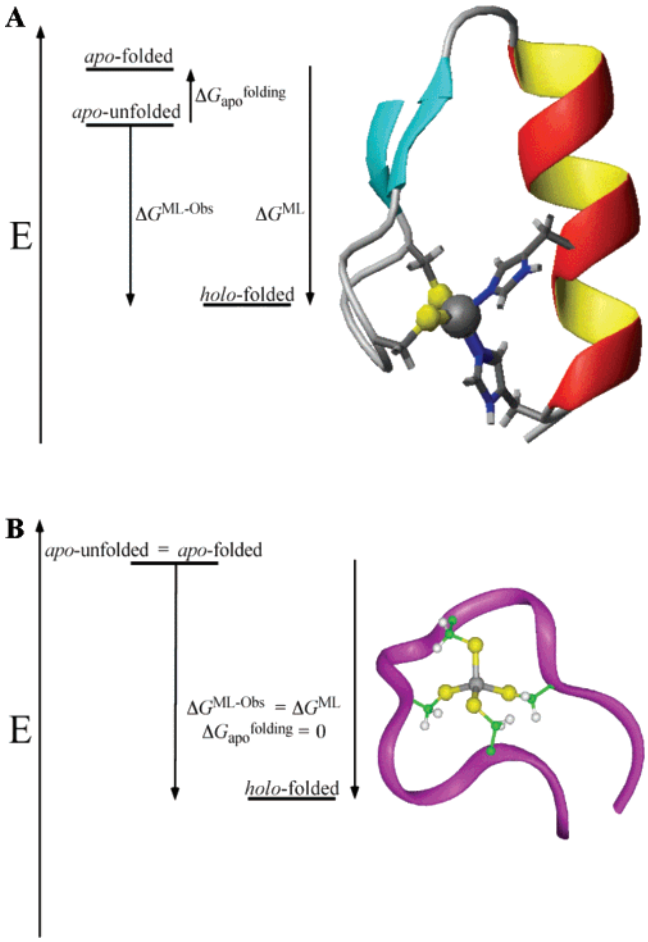

[a] (A) A coupled metal-induced protein folding event and (B) a metal binding event not coupled to protein folding.

Our approach to obtaining $\Delta G_{apo}^{folding}$ values for natural zinc fingers is to compare their ΔG^{ML-Obs} values to the ΔG^{ML-Obs} values measured in a minimal, unstructured peptide scaffold with the same metal-binding coordination motif.[31] The minimal peptide scaffold **GGG** is designed to limit the energy difference between the *apo*-folded and *apo*-unfolded states, so that the values of ΔG^{ML-Obs} and ΔG^{ML} become virtually isoenergetic, i.e., $\Delta G_{apo}^{folding} = 0$, as shown in Scheme 1B.[31] The observed Zn(II) binding constants of natural zinc fingers with the same coordination motif are expected to be weaker than those of the designed peptide by the cost of protein folding, i.e., ΔG^{ML}-(**GGG**) = ΔG^{ML-Obs}(**GGG**) = ΔG^{ML-Obs}(zinc finger) − $\Delta G_{apo}^{folding}$(zinc finger). In addition, since $\Delta G_{apo}^{folding}$ approaches zero in the designed peptide, it should possess the tightest Zn(II) affinity possible for its coordination motif.

In an effort to minimize $\Delta G_{apo}^{folding}$, we have designed a 16 amino acid peptide containing four cysteine residues, **GGG**-Cys_4 or NH_2-KL**C**EGG·**C**GG**C**GG**C**·GGW-$CONH_2$, which does not form any secondary structural elements in either the *apo* or *holo* states.[31,48] Using a combination of potentiometric pH and Zn(II) titrations into **GGG**-Cys_4, the value of the pH independent formation constant, K_f^{ML}, of the Zn(II)-**GGG**-Cys_4 complex was determined to be 1.7×10^{16} M^{-1}, or a K_d value of 60 attomolar.[31] This value is the tightest formation constant

(43) Costello, A. L.; Periyannan, G.; Yang, K.-W.; Crowder, M. W.; Tierney, D. L. *J. Biol. Inorg. Chem.* **2006**, *11*, 351−358.
(44) Sixpack is available free of charge from http://www-ssrl.slac.stanford.edu/~swebb/index.htm.
(45) Clark-Baldwin, K.; Tierney, D. L.; Govindaswamy, N.; Gruff, E. S; Kim, C.; Berg, J.; Koch, S. A.; Penner-Hahn, J. E. *J. Am. Chem. Soc.* **1998**, *120*, 8401−8409.
(46) Thomas, P. W.; Stone, E. M.; Costello, A. L.; Tierney, D. L.; Fast, W. *Biochemistry* **2005**, *44*, 7559−7565.
(47) Pavletich, N. P.; Pabo, C. O. *Science* **1991**, *252*, 809−817.
(48) Gibney, B. R.; Mulholland, S. E.; Rabanal, F.; Dutton, P. L. *Proc. Natl. Acad. Sci. U.S.A.* **1996**, *93*, 15041−15046.

measured for a Zn(II) peptide or protein to date, consistent with our ability to minimize the cost of protein folding in this scaffold, $\Delta G_{apo}^{folding}$.

As expected, Zn(II)-**GGG**-Cys_4 formation thermodynamics are highly pH dependent below the pK_a values of the ligands. At pH 7.0, reaction of $\{Zn(II)(H_2O)_6\}^{2+}$ with **GGG**-Cys_4 to form Zn(II)-**GGG**-Cys_4 is favorable, $\Delta G°$ of -15.1 kcal/mol; enthalpically disfavored, $\Delta H°$ of $+6.4$ kcal/mol; and entropy driven, $-T\Delta S°$ of -21.5 kcal/mol.[31] The unfavorable enthalpy is due in part to breaking the six Zn(II)$-H_2O$ bonds and the four cysteine S$-$H bonds, while the favorable entropy that dominates the reaction energetics is due to the release of protons and water from the reactants.

A comparison of the ΔG^{ML-Obs} value of Zn(II)-**GGG**-Cys_4 to the range of reported ΔG^{ML-Obs} values for zinc proteins with Cys_4 coordination motifs can be used to estimate the value of $\Delta G_{apo}^{folding}$ in the latter.[31] This analysis of the free energy cost of protein folding in Zn(II)-Cys_4 proteins showed that the thermodynamic barrier to folding a zinc finger protein is not as costly as the $+16$ kcal/mol predicted by Blaise and Berg, but much smaller, $\sim +4$ kcal/mol, and even negligible in one case, giving rise to the possibility that Zn(II) may kinetically template[49] the folding process for certain metalloproteins.

In this contribution, we extend this analysis of natural zinc finger $\Delta G_{apo}^{folding}$ values to include proteins with Zn(II)-Cys_3His_1 and Zn(II)-Cys_2His_2 sites. We utilize the Cys_3His_1 and Cys_2His_2 variants of **GGG**-Cys_4 to maintain the minimal cost of folding the model scaffold. Using equilibrium measurements analogous to those described for Zn(II)-**GGG**-Cys_4, we determine both the pH dependent conditional dissociation constants, K_d values, and the pH independent formation constant, K_f^{ML}, for Zn(II)-**GGG**-Cys_3His_1 and Zn(II)-**GGG**-Cys_2His_2. These data are used to show that the cost of protein folding in natural zinc finger proteins is minimal compared to the free energy contribution of Zn(II) binding, regardless of the Zn(II) coordination motif. In addition, ITC measurements conducted as a function of pH are used to determine the role of protons in modulating the reaction thermodynamics. These data reveal that proton-based enthalpy$-$entropy compensation (H^+-EEC) is responsible for the observation that zinc binding constants of natural zinc finger proteins are relatively invariant despite Cys to His alterations in their coordination spheres.[15]

Isothermal Titration Fluorimetry. The fluorescence profiles of *apo*- and *holo*- **GGG**-Cys_3His_1 and **GGG**-Cys_2His_2 are similar to that previously reported for **GGG**-Cys_4.[31] The 355 nm fluorescence emission maximum, λ_{max}^{em}, of the *apo*- and *holo*-**GGG** variants are indicative of a solvent exposed tryptophan.[50] The fluorescence emission intensity increases by $\sim$30% upon addition of 1.0 equiv of Zn(II) and can be returned to its initial *apo*-peptide intensity upon removal of the Zn(II) by addition of an excess of the metal chelator EDTA. The increase in tryptophan fluorescence emission was used to determine the conditional equilibrium dissociation constants for each peptide from Zn(II) binding isotherms. Figure 1A shows the fluorescence emission spectra of 17 μM *apo*-**GGG**-Cys_3His_1 upon titration with Zn(II) in aqueous buffer at pH 5.5 (20 mM MES, 100 mM KCl) which is representative of the series.

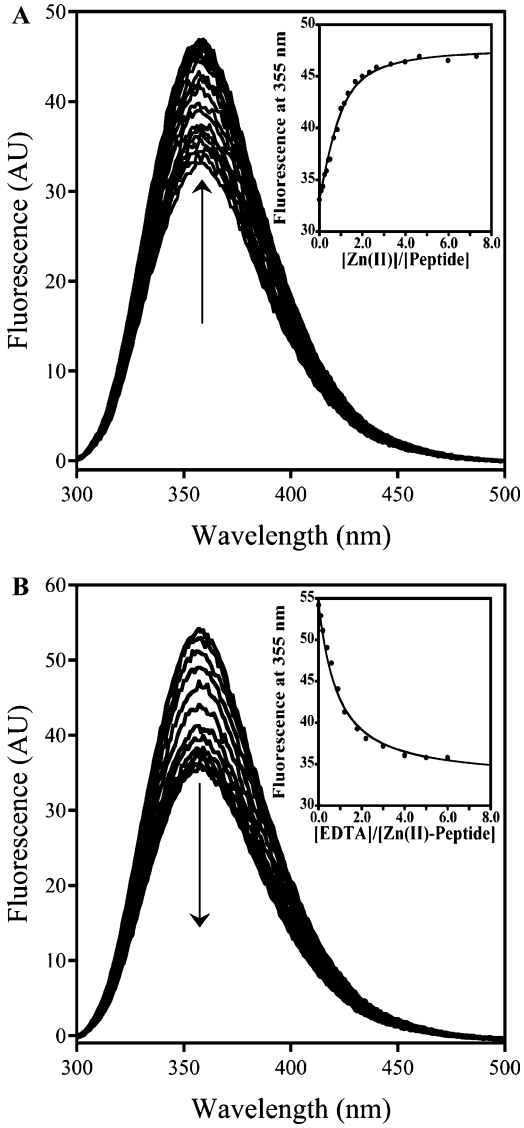

Figure 1. Fluorimetric determination of Zn(II)-**GGG**-Cys_3His_1 K_d values. (A) Fluorescence emission spectra of 17 μM *apo*-peptide upon titration with $ZnCl_2$ at pH 5.5 and binding isotherm fit to a K_d value of 5.0 μM (inset). (B) Fluorescence emission spectra of 10 μM Zn(II)-**GGG**-Cys_3His_1 upon titration with EDTA at pH 8.0 and competition isotherm fit to a K_d value of 2.5 fM (inset).

The inset shows a plot of the increase in fluorescence emission intensity at 355 nm as a function of the molar ratio of Zn(II) to peptide. The data at pH 5.5 are fit to a 1:1 binding model with a conditional dissociation constant, K_d, value of 5.0 μM.

Since Zn(II) binding is coupled to proton release, we measured the pH dependence of the conditional dissociation constant for Zn(II)-**GGG**-Cys_3His_1 and Zn(II)-**GGG**-Cys_2His_2 in a manner analogous to that previously reported for Zn(II)-**GGG**-Cys_4.[31] Conditional dissociation constant determinations for both Zn(II)-**GGG**-Cys_3His_1 and Zn(II)-**GGG**-Cys_2His_2 between pH 4.5 and 6.0 were accomplished by direct $ZnCl_2$ titration into buffered peptide solutions as described above. In each case, the data are fit to a 1:1 binding model to obtain the conditional dissociation constants.

At pH values between 6.0 and 9.0, accurate K_d determinations necessitated the use of EDTA as a competing chelator. Figure 1B shows the equilibrium competition titration between EDTA and Zn(II)-**GGG**-Cys_3His_1 in pH 8.0 buffer (20 mM HEPES,

(49) Vilar, R. *Struct. Bonding* **2004**, *111*, 85$-$137.
(50) Lakowicz, J. R. *Principles of Fluorescence Spectroscopy*; Kluwer Academic: New York, 1999.

100 mM KCl), which is representative of the series. The resulting binding isotherm shows the loss of tryptophan fluorescence emission due to the transfer of Zn(II) from Zn(II)-**GGG**-Cys_3His_1 to EDTA. The data are fit to a model that yields an equilibrium competition constant, K_{comp}, value of 2.0. Since the K_d value of Zn(II)-EDTA at pH 8.0 is 5.0 fM,[33] the K_{comp} value of 2.0 indicates that Zn(II)-**GGG**-Cys_3His_1 has a K_d value of 2.5 fM at pH 8.0.

UV/vis/NIR Spectroscopy of Co(II)-Substituted GGG-Cys_4, GGG-Cys_3His_1, and GGG-Cys_2His_2. Co(II) was incorporated into each **GGG** variant since Co(II) complexes show distinctive UV/vis spectra that are sensitive to the coordination geometry and ligand type.[51,52] Figure 2A−C shows that titration of $CoCl_2$ into aqueous buffered (20 mM HEPES, 100 mM KCl, pH 7.5) solutions of **GGG**-Cys_4, **GGG**-Cys_3His_1, and **GGG**-Cys_2His_2 result in characteristic charge transfer and ligand field electronic transitions, summarized in Table 2, indicative of a pseudo-tetrahedral coordination sphere, with the appropriate number of thiolate ligands.[51−54] The insets, plots of the extinction coefficient at the λ_{max} of the S → Co(II) charge-transfer band vs equivalents of Co(II) added relative to peptide, show tight formation of 1:1 Co(II)−peptide complexes, with conditional dissociation constants, K_d values, tighter than 500 nM at pH 7.5. Furthermore, the Racah parameters (*B* values) and tetrahedral field splitting energies, Δ_t, for each Co(II)-**GGG** variant, which were determined from the energies of the $^4A_2 \rightarrow {}^4T_1(F)$ and $^4A_2 \rightarrow {}^4T_1(P)$ vis/NIR d−d electronic transitions, given in the Supporting Information and summarized in Table 2, are similar to a series of Co(II)-substituted $Cys_{4-x}His_x$ designed zinc finger peptides.[20,53] As expected based on the relative positions of thiolate and imidazole in the spectrochemical series, Δ_t increases linearly with the number of histidine ligands present.[53]

In toto, the UV/vis/NIR spectroscopy of the Co(II)-substituted **GGG** peptides indicates that each forms a 1:1 complex with Co(II) bound in pseudo-tetrahedral coordination geometry with the appropriate number of thiolate and imidazole ligands.

X-ray Absorption Spectroscopy of Zn(II)-substituted GGG-Cys_4, GGG-Cys_3His_1, and GGG-Cys_2His_2. X-ray absorption spectroscopy was used to verify the Zn coordination spheres in the series of **GGG** peptides. The XANES spectra (not shown) show the same minimal trends as a similar set of consensus zinc finger peptides and related model complexes reported previously.[45] The edge energies (first inflection points) vary little, ranging from 9661.5 (**GGG**-Cys_2His_2) to 9662.0 eV (**GGG**-Cys_4). As shown in Figure 3, the EXAFS is dominated by metal−sulfur scattering; the main peak in the Fourier transformed EXAFS progresses linearly to a longer distance and higher intensity with increasing thiolate coordination. The main peak also sharpens as the Zn(II) coordination sphere becomes more homogeneous. The **GGG**-Cys_3His_1 and **GGG**-Cys_2His_2 complexes also show the distinctive outer-shell scattering associated with imidazole coordination.

To directly compare the primary coordination sphere in the current set to the preceding consensus zinc finger studies, we constructed P_i (%-improvement) vs composition plots,[45] where

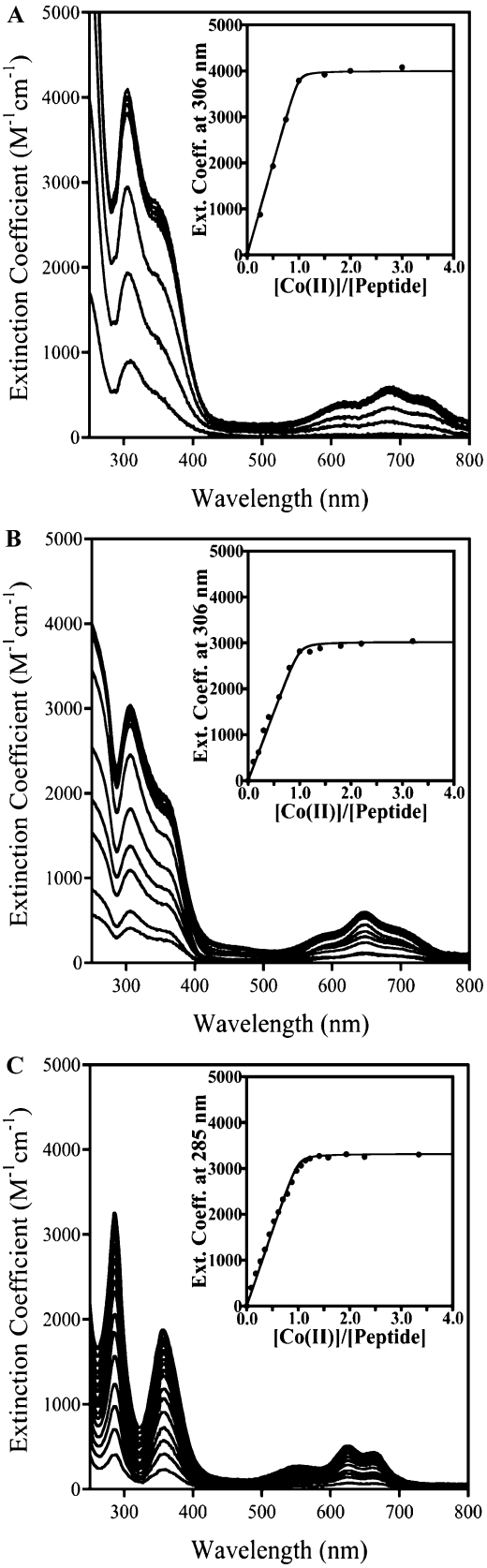

Figure 2. UV/visible determination of Co(II) substituted (A) **GGG**-Cys_4, (B) **GGG**-Cys_3His_1, and (C) **GGG**-Cys_2His_2 K_d values. The insets show tight formation of 1:1 Co(II)−peptide complexes.

P_i is defined as $P_i = (F_{2S+2S} - F_i)/F_{4S} \times 100\%$. This methodology was originally developed for the detection of small atoms in the presence of multiple larger-atom scatterers, e.g.,

(51) Lever, A. B. P. *Inorganic Electronic Spectroscopy*; Elsevier: Amsterdam, 1984.
(52) Bertini, I.; Luchinat, C. *Adv. Inorg. Chem.* **1984**, *6*, 71−111.
(53) Krizek, B. A.; Merkle, D. L.; Berg, J. M. *Inorg. Chem.* **1993**, *32*, 937−940.
(54) Anglin, J. R.; Davidson, A. *Inorg. Chem.* **1975**, *14*, 234−237.

Table 2. Electronic Transitions and Ligand Field Parameters for the Co(II)-**GGG** Variants

	Cys_4	Cys_3His_1	Cys_2His_2
Electronic Transitions			
S → Co(II) CT transitions nm (M^{-1} cm^{-1})	306 (4100)	306 (3000)	285 (3400)
	345 (2750)	355 (1900)	357 (1900)
$^4A_2 \rightarrow {}^4T_1(P)$ d−d transitions nm (M^{-1} cm^{-1})	617 (400)	590 (300)	550 (220)
	685 (650)	645 (585)	625 (500)
	730 (500)	700 (400)	660 (430)
$^4A_2 \rightarrow {}^4T_1(F)$ d−d transitions nm (M^{-1} cm^{-1})	1370 (220)	1200 (100)	1160 (160)
Ligand Field Parameters			
Δ_t (cm^{-1})	4760	5050	5250
Racah parameter, B (cm^{-1})	680	720	750

sulfur. The analysis directly compares the effect of inclusion of a small-atom scatterer, such as nitrogen or oxygen (nS + (4 − n)N, F_i), to the effect of simply increasing the number of variable parameters (2S + 2S, F_{2S+2S}) in a Fourier-filtered first shell fit. Applied here, the comparison shows that the regularity of the primary coordination environment in the **GGG** series is indeed more "ideal" than in the consensus zinc finger peptides.[45] All efforts were made to match the data analysis conditions of the previous report (Δk, ΔR, E_0, etc.) to facilitate the comparison. Within these limits, the P_i curves for the present series, shown as an inset in Figure 3, are sharper, with larger maxima, than the preceding series. As the EXAFS parameters are calibrated to idealized model interactions, steeper maxima should indicate more regular coordination polyhedra in the **GGG** series relative to the consensus zinc finger peptide complexes, consistent with the lack of protein folding effects in the former.

The details of the curve fitting results, summarized in Table 3, further support the presence of nearly ideal coordination environments in the Zn(II)-**GGG** complexes. The Zn−S distance of 2.28 Å is invariant throughout the series and is consistent with tight binding of the cysteinate ligands. The Zn−N distances are in accord with tetrahedral Zn(II) and increase slightly from **GGG**-Cys_3His_1 (2.06 Å) to **GGG**-Cys_2His_2 (2.10 Å), reflecting the need to spatially accommodate the second imidazole ring. The best fits to the data, including imidazole multiple scattering, are shown as open diamonds in Figure 3. Overestimation of the first two multiple scattering features in the **GGG**-Cys_2His_2 fit may reflect some local asymmetry in the His coordination, but the current data cannot resolve such asymmetry.

Potentiometric pH Titrations. The pH dependent chemical speciation of *apo*- and *holo*-**GGG**-Cys_4, **GGG**-Cys_3His_1, and **GGG**-Cys_2His_2 were studied using potentiometric pH titrations. Each peptide has seven sites of protonation: the four ligands, the N-terminus, the ϵ-NH_3 group of Lys_1, and the carboxylate of Glu_4. The pK_a values for these seven sites in the *apo*- and *holo*-peptides were determined by monitoring the change in solution pH as equivalents of standardized acid were added. Since metal-ion binding is expected to shift the pK_a values of the ligands, the three pK_a values that do not shift more than 0.3 upon metal ion binding were assigned to the nonligand sites: Glu_4 (4.7), Lys_1 (10.6), and the N-terminus (10.2). The ligand pK_a values shifted by ≥2.5 pH units upon metal ion binding and were assigned based on the pK_a values of the corresponding amino acids in solution, i.e., His (6.5) and Cys (8.3).[55] In addition, since tryptophan fluorescence is sensitive to the protonation state of cysteine,[34] the *holo*-peptide cysteine pK_a^{eff} values were independently determined by potentiometric titrations of the Zn(II) complex followed by fluorescence spectroscopy. These data, provided in the Supporting Information, support the assignments of the cysteine pK_a^{eff} values.

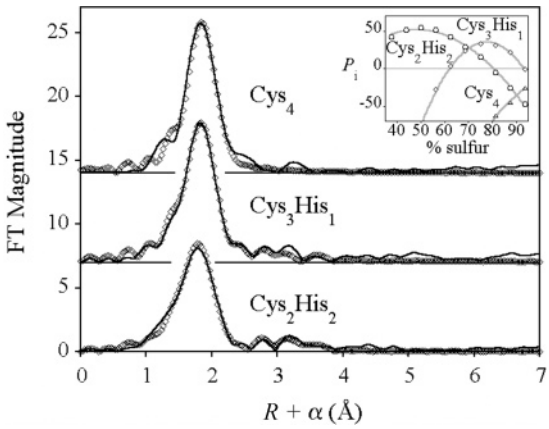

Figure 3. Fourier transformed EXAFS data (solid lines) and best fits (◇) for Zn(II)-**GGG**-Cys_4 (top), Zn(II)-**GGG**-Cys_3His_1 (center) and Zn(II)-**GGG**-Cys_2His_2 (bottom). Inset: P_i vs composition curves (the gray lines are parabolic fits included for guidance).

Figure 4A−C show the titrations of 0.1 N HCl into 100 μM *apo*- (circles) and *holo* (squares) **GGG**-Cys_4, **GGG**-Cys_3His_1, and **GGG**-Cys_2His_2 from pH 12.0 to pH 2.0. The change in solution pH of each *apo*-peptide is best fit to an equilibrium model involving seven individual protonation events. The assignments, given in Table 1, are based on a comparison of the experimental values of each peptide with the pK_a values of free amino acids in aqueous solution.[55] As expected, each replacement of a Cys with a His leads to the loss of a pK_a value near 8.3 and the addition of one near 6.5.

The change in solution pH of *holo*-**GGG**-Cys_4, Figure 4A, is best fit to an equilibrium model involving four single protonation events (Glu_4, N-terminus, Lys_1, and one Cys) and a cooperative three proton event involving three of the cysteine ligands. The assignment of the metal-bound cysteine pK_a^{eff} values (5.0 and 5.6) and their proton stoichiometry was confirmed by the fluorescence detected pH titration. As expected, the metal coordinating cysteine residues shift their pK_a^{eff} values by ≥2.5 pH units and the noncoordinating residues show less than a 0.3 pH unit shift upon metal ion binding.

The change in solution pH of *holo*-**GGG**-Cys_3His_1, Figure 4B, is best fit to a model involving five events, four single proton events (Glu_4, His_3, the N-terminus, and Lys_1), and a cooperative three proton event. The cooperative three proton pK_a^{eff} value of 5.6 is assigned to the cysteine ligands by a fluorescence detected pH titration, shown in the Supporting Information, and is similar to the pK_a^{eff} values measured for the natural Cys_3-His_1 zinc proteins HIV-1 nucleocapsid protein and primase.[56,57] As expected, the His value is observed to shift by 2.5 pH units upon Zn(II) coordination.

In the case of *holo*-**GGG**-Cys_2His_2, Figure 4C, the change in solution pH as a function of acid added is fit to six pK_a values,

(55) Mathews, C. K.; Van Holde, K. E. *Biochemistry*; Benjamin/Cummings Publishing Company: Menlo Park, CA, 1996.
(56) Bombarda, E.; Cherradi, H.; Morellet, N.; Roques, B. P.; Mély, Y. *Biochemistry* **2002**, *41*, 4312−4320.
(57) Griep, M. A.; Adkins, B. J.; Hromas, D.; Johnson, S.; Miller, J. *Biochemistry* **1997**, *36*, 544−553.

Table 3. EXAFS Curve Fitting Results for the Zn(II)-**GGG** Variants[a]

ligand set	model	Zn–S	Zn–N/O	Zn–His[b]	R_f[c]	R_u
Cys_4	4S	2.28 (4.5)	NA	NA	90	207
	2S + 2S	2.22 (0.0) 2.34 (0.0)	NA	NA	40	173
Cys_3His_1	3S + 1N	2.28 (3.6)	2.06 (2.3)	NA	14	237
	2S + 2S	2.25 (2.9) 2.31 (3.1)	NA	NA	37	258
	3S + 1N + 1His	2.27 (2.8)	2.08 (4.3)	2.94 (10), 3.11 (5.2) 3.98 (8.7), 4.31 (10)	19	138
Cys_2His_2	2S + 2N	2.28 (2.8)	2.10 (2.4)	NA	4	216
	2S + 2S	2.25 (4.4) 2.33 (8.2)	NA	NA	25	236
	2S + 2N + 2His	2.28 (2.8)	2.10 (2.6)	2.94 (16), 3.18 (6.2) 4.08 (13), 4.47 (21)	23	135

[a] Distances (Å) and disorder parameters (in parentheses, σ^2 (10^{-3} Å^2)) shown derived from integer coordination number fits to filtered EXAFS data. [b] Multiple scattering paths represent combined scattering paths described in Material and Methods. [c] Goodness of fit (R_f for fits to filtered data, R_u for fits to unfiltered data) defined as $1000 \times (\sum_{i=1}^{N} \{[\mathrm{Re}(\chi^i_{calcd})^2] + [\mathrm{Im}(\chi^i_{calcd})^2]\})/(\sum_{i=1}^{N} \{[\mathrm{Re}(\chi^i_{obs})^2] + [\mathrm{Im}(\chi^i_{obs})^2]\})$, where N is the number of data points. $\Delta k = 2.0 - 12.0$ Å^{-1}; $\Delta R = 0.8 - 2.4$ Å for first shell fits; $\Delta R = 0.1 - 4.5$ Å for multiple scattering fits.

five single proton events (Glu_4, His_3, His_7, the N-terminus, and Lys_1), and a cooperative two proton protonation for the two Cys residues. As above, the cooperative two proton event assigned to the cysteine pK_a^{eff} value was also observed via fluorescence detected pH titrations, shown in the Supporting Information, and each ligand, His or Cys, shows a pK_a shift of ≥2.0 pH units upon metal ion binding.

Analysis of the Conditional Dissociation Constant pH Dependence. The pH dependencies of the conditional dissociation constants, K_d values, of the Zn(II)-**GGG** complexes, shown in Figure 5, were analyzed to yield their pH independent formation constant values, K_f^{ML}. The binding affinity at any given solution pH is governed by the speciation of the *apo*- and *holo*-peptide, as well as the metal hydrate. The potentiometric pH titrations of the *apo*- and *holo*-**GGG** variants, described above, define the chemical speciation of the *apo*- and *holo*-peptides, with $\{Zn(II)(H_2O)_6\}^{2+}$ being the predominant metal species below pH 9.0.[40,41] Scheme 2 shows the minimal equilibrium models used to determine the values of K_f^{ML} for (A) Zn(II)-**GGG**-Cys_4, (B) Zn(II)-**GGG**-Cys_3His_1, and (C) Zn(II)-**GGG**-Cys_2His_2. These equilibrium models, which relate the Zn(II)−peptide complex K_d values over a broad pH range, include the pK_a and pK_a^{eff} values of the ligands determined potentiometrically, as well as the pH independent formation constants of the metal−peptide complexes, K_f^{ML} and $K_f^{MLH_4}$. The pK_a values of Glu_4, the N-terminus, and Lys_1 are excluded from this analysis since they do not shift significantly upon Zn(II) binding and, hence, do not contribute toward the Zn(II) binding affinity.

Previously, we reported a pH independent formation constant, K_f^{ML}, of 1.7×10^{16} M^{-1}, or a limiting K_d value of 60 attomolar at high pH for the Zn(II)-**GGG**-Cys_4 complex.[31] Redetermination of the *holo*-peptide pK_a^{eff} values by potentiometry, presented in Figure 4A, results in a slightly tighter pH independent formation constant, K_f^{ML}, of 5.6×10^{16} M^{-1}, or a limiting K_d value of 18 attomolar at high pH, as shown in Figure 5. Analysis of the data in Figure 5 for Zn(II)-**GGG**-Cys_3His_1 yields a K_f^{ML} value of 1.5×10^{15} M^{-1} and a limiting K_d value of 0.7 femtomolar. This K_f^{ML} value indicates that Zn(II) binding to **GGG**-Cys_3His_1 contributes −20.7 kcal/mol to metalloprotein stability since $\Delta G^{ML-Obs} = RT \ln K_f^{ML}$. This −20.7 kcal/mol contribution in Zn(II)-**GGG**-Cys_3His_1 is +2.1 kcal/mol, or a factor of 33, weaker than the −22.8 kcal/mol stabilization afforded by the Cys_4 coordination sphere in Zn(II)-**GGG**-Cys_4. A similar +2.4 kcal/mol effect is observed for replacement of a second cysteine with a histidine. Figure 5 also shows that the K_f^{ML} of Zn(II)-**GGG**-Cys_2His_2 is 2.5×10^{13} M^{-1}, with a limiting K_d value of 40 femtomolar, and a −18.3 kcal/mol contribution toward metalloprotein stability. These results are consistent with literature precedent that cysteine thiolates are better ligands for Zn(II) than neutral histidine imidazoles[16−18] and demonstrate that each Cys to His modification results in about a 2.0 kcal/mol destabilization at high pH. Furthermore, the limiting K_d values of the designed peptides are as tight or tighter than the observed K_d values for natural zinc finger proteins with the same coordination motif,[56−73] consistent with equivalent ΔG^{ML-Obs} and ΔG^{ML} values in the former.

Isothermal Titration Calorimetry. In order to determine the enthalpic and entropic contributions to the free energies of Zn(II) binding to **GGG**-Cys_4, **GGG**-Cys_3His_1, and **GGG**-Cys_2His_2, we employed isothermal titration calorimetry (ITC). Since the speciation of these complexes is highly pH dependent, we measured the enthalpy of Zn(II) complexation at four different pH values, pH = 5.5, 7.0, 7.4, and 8.0. These conditions were chosen to facilitate direct comparison to the data previously reported for Zn(II)-**GGG**-Cys_4.[31] At pH 5.5, where the equilibrium binding constants for Zn(II)-**GGG**-Cys_3His_1 and Zn(II)-**GGG**-Cys_2His_2 could be directly measured by ITC, the

(58) Bal, W.; Schwerdtle, T.; Hartwig, A. *Chem. Res. Toxicol.* **2003**, *16*, 242−248.
(59) Roehm, P. C.; Berg, J. M. *Biochemistry* **1997**, *36*, 10240−10245.
(60) Payne, J. C.; Rous, B. W.; Tenderholt, A. L.; Godwin, H. A. *Biochemistry* **2003**, *42*, 14214−14224.
(61) Green, L. M.; Berg, J. M. *Proc. Natl. Acad. Sci. U.S.A.* **1989**, *86*, 4047−4051.
(62) Green, L. M.; Berg, J. M. *Proc. Natl. Acad. Sci. U.S.A.* **1990**, *87*, 6403−6407.
(63) (a) Berkovits, H. J.; Berg, J. M. *Biochemistry* **1999**, *38*, 16826−16830. (b) Berkovitz-Cymet, H. J.; Amann, B. T.; Berg, J. M. *J. Am. Chem. Soc.* **2004**, *43*, 898−903.
(64) Bombarda, E.; Cherradi, H.; Morellet, N.; Roques, B. P.; Mély, Y. *Biochemistry* **2002**, *41*, 4312−4320.
(65) Bavoso, A.; Ostuni, A.; Battistuzzi, G.; Menabue, L.; Saladini, M.; Sola, M. *Biochem. Biophys. Res. Commun.* **1998**, *242*, 385−389.
(66) Posewitz, M. C.; Wilcox, D. E. *Chem. Res. Toxicol.* **1995**, *8*, 1020−1028.
(67) Berg, J. M.; Merkle, D. L. *J. Am. Chem. Soc.* **1989**, *111*, 3759−3761.
(68) Lachenmann, M. J.; Ladbury, J. E.; Dong, J.; Huang, K.; Carey, P.; Weiss, M. A. *Biochemistry* **2004**, *43*, 13910−13925.
(69) Lachenmann, M. J.; Ladbury, J. E.; Phillips, N. B.; Narayana, N.; Qian, X.; Weiss, M. A. *J. Mol. Biol.* **2002**, *316*, 969−989.
(70) Hori, Y.; Sugiura, Y. *J. Am. Chem. Soc.* **2002**, *124*, 9362−9363.
(71) McLendon, G.; Hull, H.; Larkin, K.; Chang, W. *J. Biol. Inorg. Chem.* **1999**, *4*, 171−174.
(72) Kou, W.; Kolla, H. S.; Ortiz-Acevedo, A.; Haines, D. C.; Junker, M.; Dieckmann, G. R. *J. Biol. Inorg. Chem.* **2005**, *10*, 167−180.
(73) Mély, Y.; Cornille, F.; Fournie-Zaluski, M.; Darlix, J.; Roques, B. P.; Gérard, D. *Biopolymers* **1991**, *31*, 899−906.

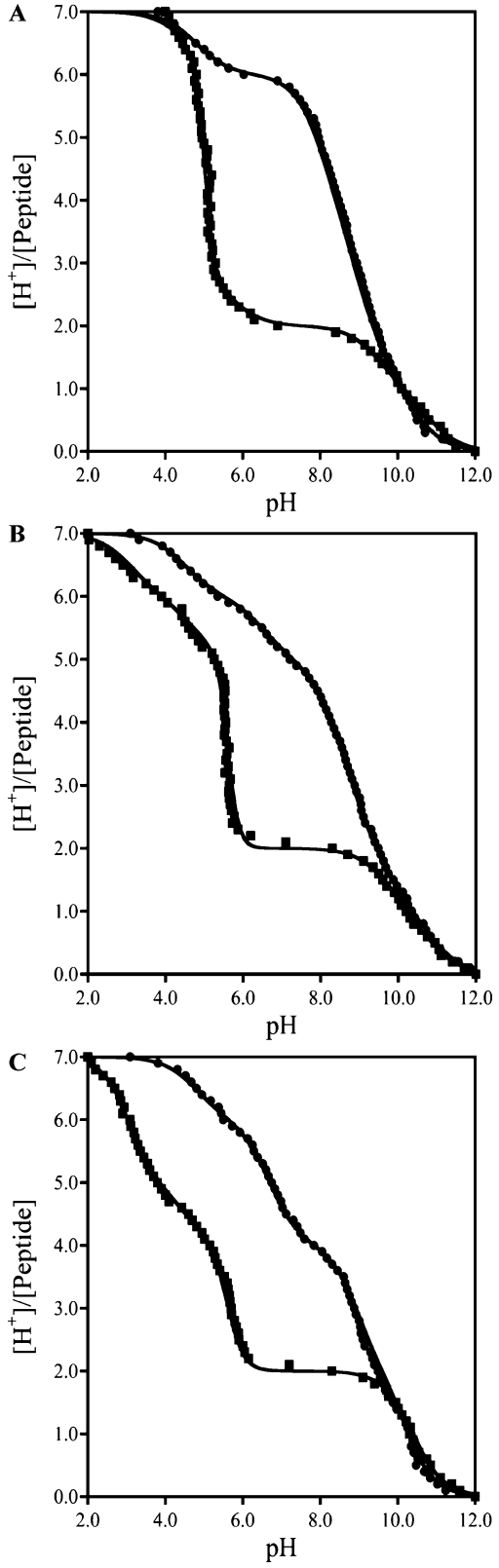

Figure 4. Potentiometric pH titrations of *apo*- (●) and *holo*- (■) (A) **GGG**-Cys_4, (B) **GGG**-Cys_3His_1, and (C) **GGG**-Cys_2His_2.

thermogram and binding isotherm provide the reaction enthalpy and free energy, respectively, thus providing the reaction entropy according to eq 2. At pH 7.0, 7.4, and 8.0, the metal-binding equilibria were too tight to measure accurately by ITC, so the

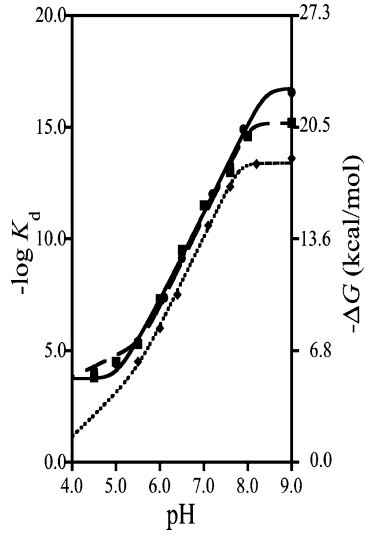

Figure 5. pH dependence of the conditional dissociation constants, K_d values, for Zn(II)-**GGG**-Cys_4 (●, solid line), Zn(II)-**GGG**-Cys_3His_1 (■, dotted line), and Zn(II)-**GGG**-Cys_2His_2 (◆, dashed line).

Scheme 2 Minimal Equilibrium Models Used To Fit the pH Dependence of the Free Energy of Zn(II) Complexation

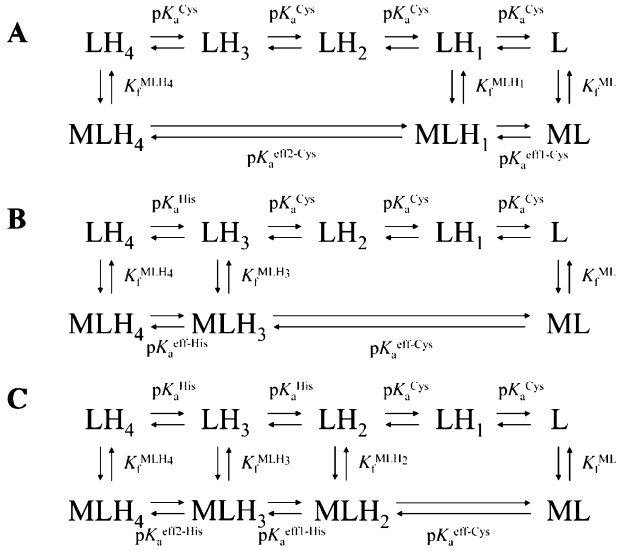

[a] (A) **GGG**-Cys_4, (B) **GGG**-Cys_3His_1, and (C) **GGG**-Cys_2His_2.

ITC determined reaction enthalpy was coupled with the reaction free energy determined by fluorimetry to yield the reaction entropy.

Figure 6 shows a representative thermogram and equilibrium binding isotherm of $ZnCl_2$ titrated into 50 μM **GGG**-Cys_3His_1 at pH 5.5 where the speciation equilibria given in Scheme 2 indicate release of 2.0 protons upon Zn(II) complexation. The binding isotherm shows the expected 1:1 stoichiometry and a fit of the data to a 1:1 binding model yields a conditional K_d value of 25 μM ($\Delta G_{rxn} = -6.3$ kcal/mol). This conditional K_d value is identical within error to that determined by fluorimetry under the same conditions, shown in Figure 1A, demonstrating that both experimental techniques yield comparable results. After correcting for the enthalpy due to the loss of 2.0 protons, ΔH_{rxn} was determined to be +3.2 kcal/mol, ΔG_{rxn}, to be −7.2 kcal/mol, and $-T\Delta S_{rxn}$, to be −10.4 kcal/mol at 25 °C. Thus, Zn(II) complexation by **GGG**-Cys_3His_1 is favorable, endothermic, and entropically driven at pH 5.5.

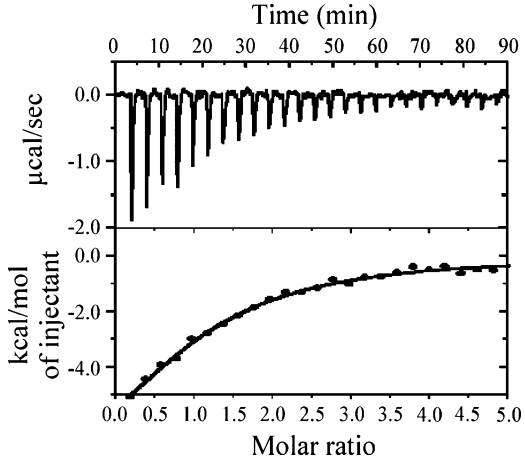

Figure 6. A thermogram and equilibrium binding isotherm of $ZnCl_2$ titrated into 50 μM **GGG**-Cys_3His_1 at pH 5.5. The binding isotherm is fit to a K_d value of 25 μM.

At pH 7.0, where the speciation equilibria given in Scheme 2 indicate release of 3.2 protons upon Zn(II) binding, the isotherm shows the expected 1:1 stoichiometry but only provides a weak limit of the conditional K_d value. After correcting for the loss of 3.2 protons at pH 7.0, ΔH_{rxn} was determined to be +3.7 kcal/mol. This value was coupled with the fluorimetrically derived ΔG_{rxn} of −15.0 kcal/mol to calculate a $-T\Delta S_{rxn}$ value of −18.7 kcal/mol at 25 °C. Thus, at pH 7.0, Zn(II) complexation by **GGG**-Cys_3His_1 remains favorable, endothermic, and entropically driven. Similar analyses at pH 7.4 and 8.0, where 2.9 and 2.3 protons are released, yield ΔH_{rxn} values of +1.0 and −4.3 kcal/mol, ΔG_{rxn} values of −17.3 and −20.0 kcal/mol, and $-T\Delta S_{rxn}$ values of −18.3 and −15.7 kcal/mol at 25 °C, respectively. Thus, as solution pH increases, the reaction becomes more enthalpically favorable and less entropically driven.

The results of analogous experiments on Zn(II) binding to **GGG**-Cys_2His_2 are presented in Table 4 and summarized here. Zn(II) complexation by **GGG**-Cys_2His_2 at pH 5.5 is favorable by −6.2 kcal/mol (ΔG_{rxn}), endothermic by +3.7 kcal/mol (ΔH_{rxn}) after accounting for the release of 2.7 protons, and entropically driven by −9.9 kcal/mol at 25 °C ($-T\Delta S_{rxn}$). At pH 7.0, the reaction of $\{Zn(II)(H_2O)_6\}^{2+}$ with **GGG**-Cys_2His_2 is −14.0 kcal/mol favorable (ΔG_{rxn}), +3.3 kcal/mol endothermic (ΔH_{rxn}), releases 2.5 protons, and is entropically driven by −17.3 kcal/mol at 25 °C ($-T\Delta S_{rxn}$). At pH 7.4, the reaction of $\{Zn(II)(H_2O)_6\}^{2+}$ with **GGG**-Cys_2His_2 is −16.3 kcal/mol favorable (ΔG_{rxn}), −0.1 kcal/mol exothermic (ΔH_{rxn}), releases 2.2 protons, and is entropically driven by −16.2 kcal/mol at 25 °C ($-T\Delta S_{rxn}$). At pH 8.0, Zn(II) complexation by **GGG**-Cys_2His_2 was determined to be favorable by −18.1 kcal/mol (ΔG_{rxn}), exothermic by −2.9 kcal/mol (ΔH_{rxn}), releases 1.8 protons, and is entropically driven by −15.2 kcal/mol at 25 °C ($-T\Delta S_{rxn}$). Thus, as observed for the other two coordination motifs, Zn(II) binding becomes more enthalpically favorable and less entropically favorable at high pH due to partial deprotonation of the cysteine ligands in the *apo*-peptide prior to Zn(II) binding.

At pH values above 7.0, where the reaction product has fully deprotonated ligand complexed with metal, the entropic and enthalpic contributions to Zn(II) complexation track with the number of protons released for each of the **GGG** variants. At pH 7.0, where the reaction releases the most protons, all three **GGG** variants exhibit the greatest entropic contributions to Zn(II) complexation, whereas, at higher pH values, the reaction releases fewer protons and the entropic contribution is attenuated. In terms of the reaction enthalpy, partial deprotonation of the ligand at pH 8.0 prior to Zn(II) binding increases the reaction enthalpy relative to pH 7.0, where extra S−H bonds must be broken to bind Zn(II). The observed trends can be rationalized based on the enthalpic cost and entropic benefit of breaking cysteine S−H or histidine N−H bonds to release protons,[31] but other factors such as water release from the reactants also effect these thermodynamics.[74,75] Shown in the Supporting Information are plots of the reaction enthalpy and entropy for the formation of the fully deprotonated Zn(II)-**GGG** complexes as a function of the number of protons released.

Last, the temperature dependence of the reaction enthalpy at pH 7.0 yields ΔC_p values of −15 cal K^{-1} mol^{-1}, −5.0 cal K^{-1} mol^{-1}, and +20 cal K^{-1} mol^{-1} for Zn(II) complexation by **GGG**-Cys_4, **GGG**-Cys_3His_1, and **GGG**-Cys_2His_2, respectively. These values are consistent with the absence of significant structural changes in the protein scaffold upon Zn(II) coordination, as expected for a minimalist, unstructured peptide. A similar negligible ΔC_p value of 10 cal K^{-1} mol^{-1} is observed for a natural Cys_3His_1 zinc finger, HIV-1 nucleocapsid protein, which is relatively unstructured in both its *apo* and *holo* states.[71] In contrast, the designed Cys_2His_2 peptide CP-1 has a ΔC_p value of −514 cal K^{-1} mol^{-1} because it folds from an unstructured *apo*-state into a $\beta\beta\alpha$ fold upon Zn(II) coordination.[12] Thus, the negligible ΔC_p values for Zn(II) coordination by the **GGG** variants reflect the lack of significant secondary structure in both the *apo* and *holo* states, as designed.

Discussion

The thermodynamic contribution of Zn(II) binding to Cys_4, Cys_3His_1, and Cys_2His_2 sites in a minimal, unstructured peptide scaffold, **GGG**, has been evaluated as a function of solution pH. Using a suite of equilibrium measurements, the solution speciation of each *apo*-peptide and Zn(II)−peptide complex was elucidated over the pH range of 4.0 to 9.0. The data indicate pH independent formation constant values, K_f^{ML} values, of 5.6×10^{16}, 1.5×10^{15}, and 2.5×10^{13} M^{-1} for the Cys_4, Cys_3His_1, and Cys_2His_2 sites, respectively. The K_f^{ML} values are attenuated by pH due to proton competition, with all three Zn(II)−peptide complexes possessing the same conditional dissociation constant, K_d value, of 0.5 pM at pH 7.4, within a factor of 10, or 1.4 kcal/mol, error of the measurements. The K_d values of Zn(II)-**GGG**-Cys_4, Zn(II)-**GGG**-Cys_3His_1, and Zn(II)-**GGG**-Cys_2His_2 between pH 6.5 and 8.0 are compared with literature values for natural zinc finger proteins possessing metal-induced protein folding events to determine the cost of protein folding in the latter. These results indicate that the cost of protein folding in many natural zinc fingers is minimal, less than +4.2 kcal/mol, compared with the thermodynamic contribution of Zn(II) binding, greater than −15 kcal/mol. Last, proton-based entropy−enthalpy compensation (H^+-EEC) is responsible for the observed equivalence of the K_d values at pH 7.4 for the three coordination motifs: Cys_4, Cys_3His_1, and Cys_2His_2.

(74) DiTusa, C. A.; Christensen, T.; McCall, K. A.; Fierke, C. A.; Toone, E. J. *Biochemistry* **2001**, *40*, 5338−5344.
(75) DiTusa, C. A.; McCall, K. A.; Christensen, T.; Mahapatro, M.; Fierke, C. A.; Toone, E. J. *Biochemistry* **2001**, *40*, 5345−5351.

Table 4. pH Dependence of the Thermodynamics of Zn(II) Complexation by the **GGG** Variants

	Cys_4				Cys_3His_1				Cys_2His_2			
pH	5.5	7.0	7.4	8.0	5.5	7.0	7.4	8.0	5.5	7.0	7.4	8.0
ΔG_{rxn} (kcal/mol)	−7.4	−15.3	−17.4	−20.7	−7.2	−15.0	−17.3	−20.0	−6.2	−14.0	−16.3	−18.1
ΔH_{rxn} (kcal/mol)	+7.7	+6.4	+5.6	−2.0	+3.2	+3.7	+1.0	−4.3	+3.7	+3.3	−0.1	−2.9
$-T\Delta S_{rxn}$ (kcal/mol)	−15.1	−21.7	−23.0	−18.7	−10.4	−18.7	−18.3	−15.7	−9.9	−17.3	−16.2	−15.2
H^+ released	3.2	3.8	3.6	2.5	2.0	3.2	2.9	2.3	2.7	2.5	2.2	1.8

Table 5. Determination of the Cost of Protein Folding in Zinc Finger Proteins

protein	pH	protein K_d	protein ΔG^{ML-Obs} (kcal/mol)	**GGG** K_d	**GGG** ΔG^{ML-Obs} (kcal/mol)	protein $\Delta G_{apo}^{folding}$ (kcal/mol)	protein fold
				Zn(II)-Cys_4 Sites			
CP-CCCC[53]	7.0	1.1 pM	−16.3	6 pM	−15.3	−1.0[79]	$\beta\beta\alpha$
BRCA1[59]	7.0	32 pM	−14.3	6 pM	−15.3	+1.0	RING finger domain
hERα-DBD[60]	7.4	100 pM	−13.6	160 fM	−17.4	+3.8	$\beta\beta\alpha\alpha$
XPA-zf[58]	7.4	153 pM	−13.4	160 fM	−17.4	+4.0	mixed $\alpha\beta$
GR-DBD[60]	7.4	200 pM	−13.2	160 fM	−17.4	+4.2	$\beta\beta\alpha\alpha$
				Zn(II)-Cys_3His_1 Sites			
L36[72]	6.0	17 nM	−10.6	50 nM	−10.0	−0.6	3 stranded β-sheet
NZF-1[63]	6.9	125 pM	−13.5	16 pM	−14.7	+1.2	CCHHC domain
$RMLV_{protein}$[67]	7.0	1 pM	−16.4	10 pM	−15.0	−1.4	random coil
CP−CCHC[59]	7.0	3 pM	−15.7	10 pM	−15.0	−0.7	$\beta\beta\alpha$
$RMLV_{peptide}$[62]	7.0	690 pM	−12.5	10 pM	−15.0	+2.5	β turns
MoMuLV protein[61]	7.9	6.0 fM	−19.4	2.5 fM	−19.9	+0.5	random coil
Fw[65]	8.0	1.9 pM	−16.0	2.0 fM	−20.1	+4.1	unknown
HIV-1 nucleocapsid protein[64, 71]	9.0	500 aM	−20.9	700 aM	−20.7	−0.2	random coil
				Zn(II)-Cys_2His_2 Sites			
WT1-p[68]	6.5	1.9 nM	−11.9	6 nM	−11.2	−0.7	$\beta\beta\alpha$
ZFY[69]	6.5	300 nM	−8.9	6 nM	−11.2	+2.3	$\beta\beta\alpha$
CP1[20]	7.0	8.5 pM	−15.1	56 pM	−14.0	−1.1	$\beta\beta\alpha$
SP1-3[66]	7.0	690 pM	−12.5	56 pM	−14.0	+1.5	$\beta\beta\alpha$
TFIIIA[67]	7.0	10 nM	−10.9	56 pM	−14.0	+3.1	$\beta\beta\alpha$
AntF[70]	7.5	12 nM	−10.8	760 fM	−16.5	+5.7	$\beta\beta\alpha$

The formation constants of the Zn(II)-**GGG** complexes are the tightest measured to date and may represent the maximal value for their respective coordination motifs. The data show that Zn(II) binding to **GGG**-Cys_4, **GGG**-Cys_3His_1, and **GGG**-Cys_2His_2 sites contributes −22.8, −20.7, and −18.3 kcal/mol, respectively, toward metalloprotein stability. The loss of about 2.0 kcal/mol per Cys to His replacement is consistent with the cysteine thiolate being a better ligand for Zn(II) than the histidine imidazole.[16−18] However, the observed 4.5 kcal/mol span in the free energies of Zn(II) binding to the three scaffolds at pH 9.0 is attenuated to a difference of only 1.0 kcal/mol at pH 7.4 due to proton competition. The equalization in the Zn(II) binding energetics of the three coordination motifs at physiological pH is consistent with observations that zinc finger proteins, regardless of coordination sphere, have similar K_d values[15,20,53] and that interchanging Cys and His can still lead to zinc finger folding and nucleic acid binding[20,53,72,76] if the change does not result in significant structural perturbations.[77,78] Since we have designed the **GGG** scaffold to minimize the cost of protein folding, we propose that these K_f^{ML} and K_d values are the maximal values possible for their coordination motifs.

The lack of an energetic penalty for protein folding in the **GGG** scaffold is supported by a comparison of its conditional dissociation constants, K_d values, with those from natural zinc finger proteins listed in Table 5. In the case of each coordination motif, there are no examples outside the 1.4 kcal/mol error of the measurements of K_d values tighter than those observed for the Zn(II)-**GGG** scaffold.[79] In several cases, K_d values of natural zinc fingers are as tight as those measured for the Zn(II)-**GGG** scaffold, which indicates that the energetic penalty for folding the scaffolds must be equivalent. In these cases, the value of $\Delta G_{apo}^{folding}$ is close to zero based on the assertion that it is zero for the **GGG** scaffold.[31]

In cases where the K_d values of the natural zinc finger proteins is weaker than those of the designed Zn(II)-**GGG** scaffold, we ascribe the difference as being due to a positive value of $\Delta G_{apo}^{folding}$. Thus, the Zn(II) binding energy is being used to thermodynamically drive the protein folding process. The examples in Table 4 indicate that the value for $\Delta G_{apo}^{folding}$ for most zinc finger proteins is less than +4.2 kcal/mol and not as high as the +16 kcal/mol estimate.[12] This conclusion that there is a small energetic difference between the folded and unfolded states of zinc finger proteins is supported by the successful redesign of a zinc finger $\beta\beta\alpha$ fold to be stable without the Zn(II) present,[24] the lack of a large increase in Zn(II) affinity

(76) Yuichiro, H.; Suzuki, K.; Okuno, Y.; Nagaoko, M.; Futaki, S.; Sugiura, Y. *J. Am. Chem. Soc.* **2000**, *122*, 7648−7653.
(77) Julian, N.; Demene, H.; Morellet, N.; Maigret, B.; Roques, B. P. *FEBS* **1993**, *331*, 43−48.
(78) Webster, L. C.; Zhang, K.; Chance, B.; Ayene, I.; Culp, J. S.; Huang, W. J.; Wu, F. Y. H.; Ricciardi, R. P. *Proc. Natl. Acad. Sci. U.S.A.* **1991**, *88*, 9989−9993.

(79) The negative $\Delta G_{apo}^{folding}$ values in Table 5 are all within the 1.4 kcal/mol error of our measurements.

in redesigned zinc finger proteins which are folded in the *apo*-state,[22,23] molecular dynamics simulations of the unfolded state of a zinc finger which indicate that the ensemble corresponds to the native state in the average sense,[80] and recent NMR structures of *apo* and *holo* TFIIB which show that the zinc ribbon motif is preformed prior to Zn(II) complexation.[81] Thus, we conclude that only a small fraction of the total Zn(II) binding energy is used to fold natural zinc finger protein scaffolds regardless of protein fold.

There is a single example of a zinc finger protein with a $\Delta G_{apo}^{folding}$ value greater than 4.2 kcal/mol. At pH 7.5, the observed 12 nM dissociation constant of the Cys_2His_2 site in the zinc finger AntF is 5.7 kcal/mol weaker than the 760 fM K_d of Zn(II)-**GGG**-Cys_2His_2.[70] In this case, *apo*-AntF is folded into a structure distinct from the structure of the Zn(II)-protein. That is to say, the *apo*-state is neither unfolded nor partially folded into the correct fold, but rather partially folded into an incorrect fold. Thus, the larger value of $\Delta G_{apo}^{folding}$ reflects the fact that Zn(II) binding must pay the added energetic price for unfolding the incorrect fold in order to fold into the correct *holo*-fold. This situation is conceptually similar to a recent pair of designed proteins in which the *apo*-proteins fold into oligomeric α-helical bundles and addition of Zn(II) results in their conversion into monomeric $\beta\beta\alpha$ folded proteins.[27,82] While detailed analysis of their Zn(II) dissociation constants have yet to be reported, we predict that they will be significantly attenuated relative to the analogous Zn(II)-**GGG** scaffold or natural zinc fingers due to a $\Delta G_{apo}^{folding}$ value related to the stability of the *apo*-peptide helical bundle.

As observed in natural zinc finger proteins, altering the coordination motif from Cys_4 to Cys_2His_2 results in little change in the conditional dissociation constant values for the Zn(II)-**GGG** complexes at physiological pH.[15] The pH dependence of Zn(II) complexation for the three **GGG** variants shows that the 4.5 kcal/mol spread in formation constant values is attenuated by pH to within 1.0 kcal/mol of each other at pH 7.4, as shown in Figure 5. Not unexpectedly, a Cys_3His_1 site in a protein with a minimal $\Delta G_{apo}^{folding}$ value, HIV-1 nucleocapsid protein possesses a similar K_d value of 1.0 pM at pH 7.4.[56] More interestingly, the conditional dissociation constant of Zn(II)-carbonic anhydrase, with a $His_3(OH)$ site, also possesses a similar K_d value of 1.0 pM at pH 7.4.[74]

Proton-based enthalpy−entropy compensation (H^+-EEC) results in the equivalence of the K_d values for the Zn(II)-**GGG** peptides at pH 7.4. Figure 7 shows a plot of ΔH_{rxn} vs $-T_{298K}\Delta S_{rxn}$ for Zn(II) complexation by **GGG**-Cys_4, **GGG**-Cys_3His, **GGG**-Cys_2His_2, and carbonic anhydrase. The excellent correlation between the enthalpy and entropy of reaction is indicative of enthalpy−entropy compensation (EEC),[83−86] a linear free energy relationship in which the differences in free energy for a set of related chemical reactions is small compared to the differences in the enthalpy and entropy. The observed

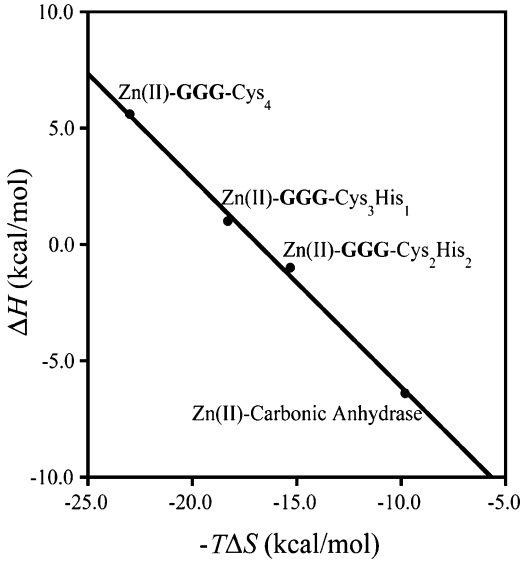

Figure 7. A plot of the enthalpy vs the entropy of zinc complexation by the **GGG** variants and carbonic anhydrase at 298 K, pH = 7.4.

EEC is due to proton management in the Zn(II)-**GGG** scaffolds. Zn(II)-**GGG**-Cys_4 formation, which releases the most number of protons, 3.6, has the greatest entropic contribution to binding, but the least enthalpic contribution, whereas **GGG**-Cys_2His_2, which releases the fewest number of protons in the series, 2.2, has the smallest entropic contribution toward Zn(II) binding and largest enthalpic contribution. **GGG**-Cys_3His_1, which releases 2.9 protons, has enthalpic and entropic contributions toward Zn(II) binding that lie between the **GGG**-Cys_4 and **GGG**-Cys_2His_2 variants, as expected based on considerations due to proton release. The calorimetric data indicate that the equalization in free energies of Zn(II) binding at pH 7.4 is due to compensation between unfavorable enthalpic terms due to S−H and/or N−H bond breakage and favorable entropic terms due to proton release. Interestingly, Zn(II)-carbonic anhydrase formation, which has a similar binding free energy to that of the **GGG** variants and releases 0.3 protons,[74] falls on the EEC line in the appropriate position, having the most favorable enthalpic contribution to binding and the least favorable entropic contribution, as expected based solely on considerations due to proton release in a protein with limited protein folding effects.

Conclusion

In the present work, we describe the thermodynamic contribution of Zn(II) binding to each of the naturally occurring zinc finger coordination motifs in a designed protein with minimal structure, **GGG**. The lack of an energetic cost of protein folding in the **GGG** scaffold results in a series of Zn(II)-proteins with the maximal formation constants for their coordination motifs. The energetic cost of folding natural zinc finger proteins appears to be minimal, ≤4.2 kcal/mol, as derived from comparisons of the conditional dissociation constants from the Zn(II)-**GGG** complexes. The data also show that the anionic cysteine thiolate is a better ligand for Zn(II) than the neutral histidine imidazole with each Cys to His alteration destabilizing the contribution of zinc binding by ∼2.0 kcal/mol. However at physiological pH, the three canonical zinc finger Zn(II) coordination sites afford similar free energy contributions toward protein stability due to proton-based enthalpy−entropy compensation.

(80) Zagrovic, B.; Snow, C. D.; Khaliq, S.; Shirts, M. R.; Pande, V. S. *J. Mol. Biol.* **2002**, *323*, 153−164.
(81) Ghosh, M.; Elsby, L. M.; Mal, T. K.; Gooding, J. M.; Roberts, S. G. E.; Ikura, M. *Biochem. J.* **2004**, *378*, 317−324.
(82) Cerasoli, E.; Sharpe, B. K.; Woolfson, D. N. *J. Am. Chem. Soc.* **2005**, *127*, 15008−15009.
(83) Sharp, K. *Protein Sci.* **2001**, *10*, 661−667.
(84) Beasley, J. R.; Doyle, D. F.; Chen, L.; Cohen, D. S.; Fine, B. R.; Pielak, G. J. *Proteins* **2002**, *49*, 398−402.
(85) Liu, L.; Guo, Q.-X. *Chem. Rev.* **2001**, *101*, 673−696.
(86) Lumry, R.; Rajender, S. *Biopolymers* **1970**, *9*, 1125−1227.

Acknowledgment. We thank Prof. Ronald Breslow for use of the isothermal titration calorimeter. This work was supported by an American Heart Association grant to B.R.G. (0755879T) and by the National Center for Research Resources (NIH) through the New Mexico INBRE program (P20 RR-16480 to D.L.T.). A.R.R. acknowledges receipt of a National Science Foundation GK-12 Graduate Fellowship (DGE-02-31875). T.R.G. acknowledges receipt of a National Science Foundation REU Fellowship (DGE-04-53178). B.R.G. is a Camille Dreyfus Teacher-Scholar. NSLS is supported by the U.S. Department of Energy.

Supporting Information Available: Derivations of the equilibrium binding models used to analyze the data, including the 1:1 binding model, the competition model, and the models used to fit the pH dependence of Zn(II) complexation by the **GGG** variants. Fluorescence detected pH titrations of Zn(II)-**GGG**-Cys_4, Zn(II)-**GGG**-Cys_3His_1, and Zn(II)-**GGG**-Cys_2His_2, and the protonation models used to fit the data. vis/NIR Spectra of the Co(II)-**GGG** complexes. Comparison of the results of the two methods used to analyze the ITC data. Plots of the enthalpy and entropy of Zn(II) complexation as a function of protons released. This material is available free of charge via the Internet at http://pubs.acs.org.

JA073902+